The Dust Emissivity Spectral Index in Cores and Filaments

Scott Schnee[1] Shadi Chitsazzadeh[2], James Di Francesco[2,3], Rachel Friesen[4], Gibion Makiwa[5], Brian Mason[1], David Naylor[5], Matthijs van der Wiel[5], Thomas Stanke[6]

[1]National Radio Astronomy Observatory, Charlottesville, VA, USA; [2]University of Victoria, Victoria, BC, Canada;
[3]National Research Council Canada, Victoria, BC, Canada;
[4]Dunlap Institute for Astronomy and Astrophysics, University of Toronto, Toronto, ON, Canada;
[5]Institute for Space Imaging Science, Dept. of Physics and Astronomy, University of Lethbridge, Lethbridge, AB, Canada
[6]European Southern Observatory, 85748, Garching, Germany

1. Introduction

Thermal dust emission is a tracer of mass within star-forming regions, so continuum maps trace the distribution of dense material involved in the star formation process. Deriving the mass from measurements of dust continuum emission is complicated by also needing to know (or simultaneously determine) the dust temperature and dust opacity. This opacity has a frequency dependence $\kappa_\nu = \kappa_0 (\nu/\nu_0)^\beta$, where β is the emissivity spectral index of dust emission.

By deriving accurate values of β, we will be able to determine more accurate core masses, temperatures, and the dust grain size distribution. Larger dust grains result in a shallower spectral energy distribution (SED), and observations of nearby protostellar disks show values of the emissivity spectral index around β=1, indicative of millimeter sized dust grains (e.g. Perez et al. 2012; Guilloteau et al. 2011). In molecular clouds, β=2 is often found (e.g. Sadavoy et al. 2013).

2. Observations of OMC-2/3

GBT MUSTANG: Observations with MUSTANG on the GBT provide us with a 3.3mm continuum map of a ~20'×5' region centered on OMC-2/3. The angular resolution is ~10", or 0.02pc at the distance of Orion.

IRAM 30m MAMBO: Observations with MAMBO on the IRAM 30m provide us with a 1.2mm continuum map of a region larger than (and including) the MUSTANG observations. The angular resolution is also ~10".

JCMT SCUBA-2/FTS-2: We have been awarded time for JCMT SCUBA-2/FTS-2 observations of OMC-2/3 from 800-900µm with coarse spectral resolution to derive a more accurate SED.

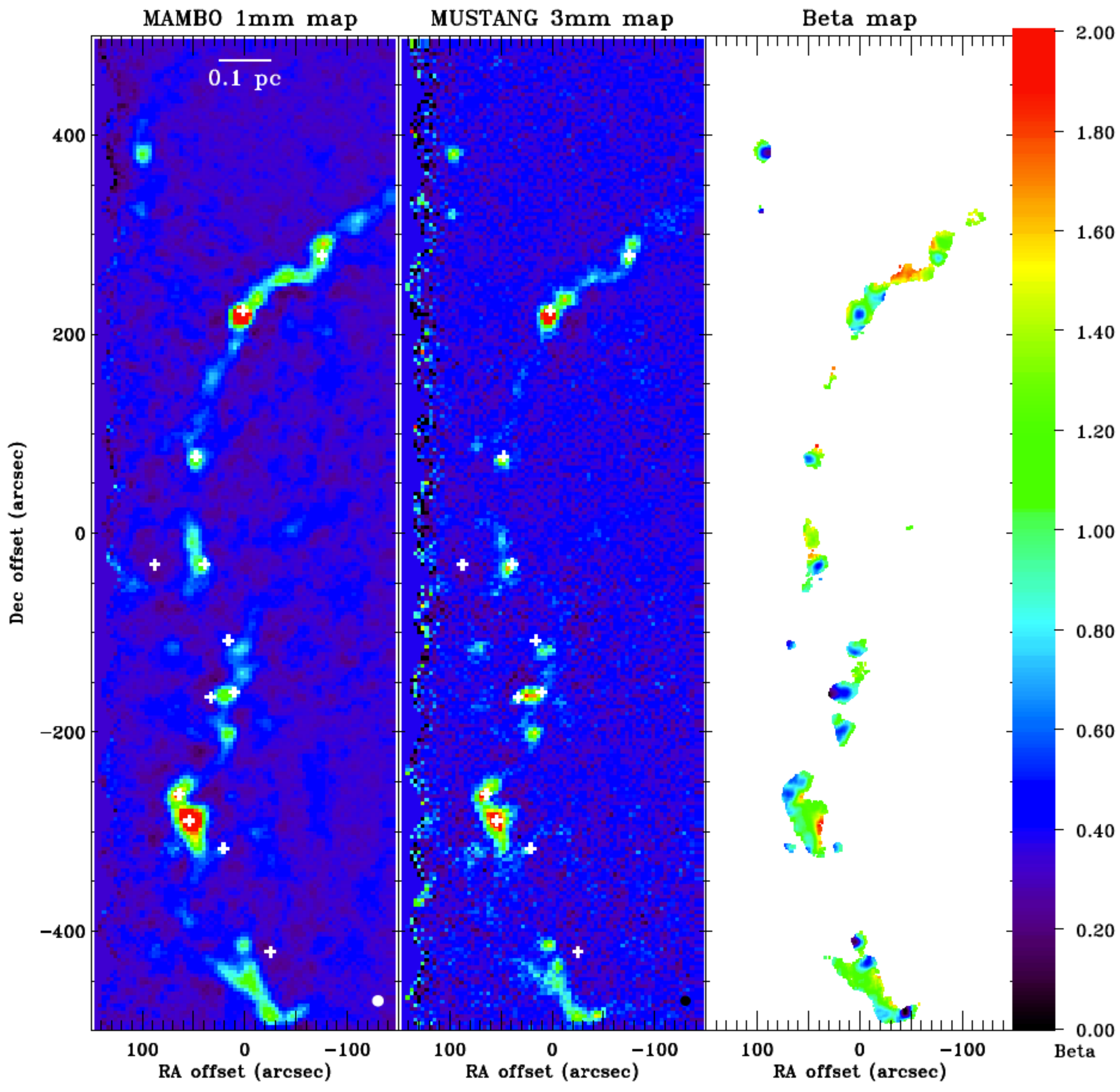

Work in progress: Derivation of β from 1mm and 3mm data
(left) 1mm MAMBO map of OMC-2/3
(*middle*) 3mm MUSTANG map of OMC-2/3
(*right*) Emissivity spectral index (β) map of OMC-2/3

3. Observations of Dense Cores

Herschel SPIRE-FTS: Observations of the dust continuum from ~200-600 µm with the Herschel/SPIRE-FTS with low spectral resolution provide us with some of the data needed to estimate the emissivity spectral index (β). These observations were taken towards a sample of 12 dense starless and protostellar cores (L694-2, L429, L183, L1517B, B18-1, B18-2, B18-4, L1507A, L1544, L1689–SMM16, L1521F, and L1014).

GBT KFPA: Observations of NH_3 (1,1) and (2,2) with the GBT KFPA towards a sample of starless and protostellar cores provide us with gas temperature maps.

JCMT SCUBA-2/FTS-2: We will use guaranteed time on the JCMT for SCUBA-2/FTS-2 800-900µm observations towards four of the dense cores already observed with SPIRE-FTS. These longer-wavelength data will allow us to make even more accurate measurements of β.

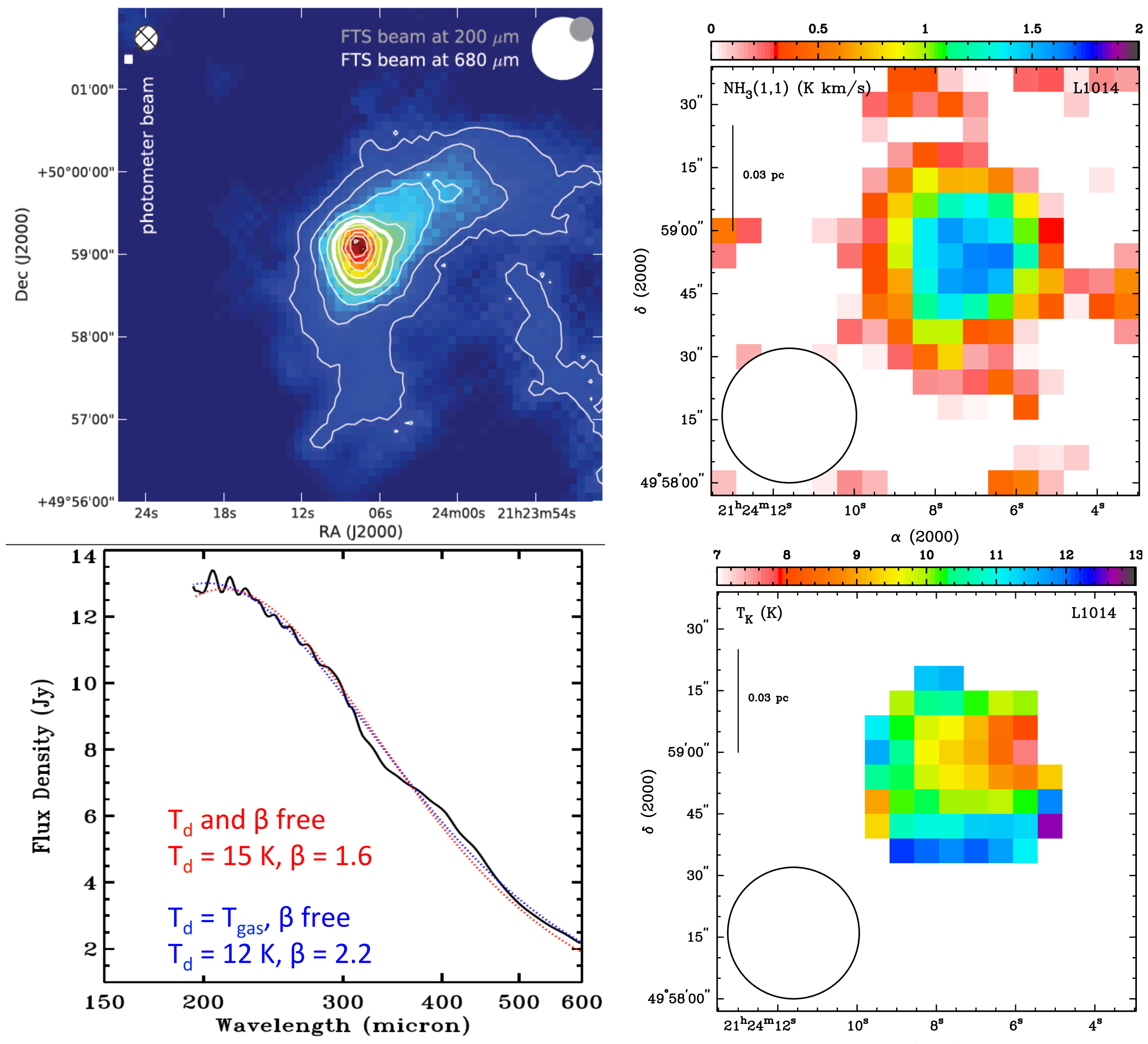

Work in progress: Derivation of β from Herschel and GBT data
(top left) Herschel SPIRE 250 µm photometric map of L1014
(top right) NH_3 (1,1) integrated intensity map of L1014
(bottom left) Herschel SPIRE-FTS SED of L1014
(bottom right) Temperature map of L1014

4. Conclusions and Future Work

OMC-2/3: The derived values of β are much lower than 2, perhaps implying grain growth on 0.1 pc scales.

Dense cores: The derived value of β in the VeLLO L1014 is 2.2, using the peak gas temperature derived from ammonia and the Herschel SPIRE-FTS spectrum at the center of the core.

5. References

- Guilloteau, Dutrey, Pietu, & Boehler 2011, A&A, 529, A105
- Perez, Carpenter, Chandler, et al., 2012, ApJL, 760, L17
- Sadavoy, Di Francesco, Johnstone et al., 2013, ApJ, 767, 126